




Article

Calcium and Strontium Coordination Polymers as Controlled Delivery Systems of the Anti-Osteoporosis Drug Risedronate and the Augmenting Effect of Solubilizers

Maria Vassaki ¹, Christina Kotoula ¹, Petri Turhanen ² , Duane Choquesillo-Lazarte ³ 
and Konstantinos D. Demadis ^{1,*} 

¹ Crystal Engineering, Growth and Design Laboratory, Department of Chemistry, University of Crete, GR-71003 Heraklion, Greece; vassakimar@gmail.com (M.V.); kotoulachris@gmail.com (C.K.)

² School of Pharmacy, University of Eastern Finland, Biocenter Kuopio, P.O. Box 1627, FIN-70211 Kuopio, Finland; petri.turhanen@uef.fi

³ Laboratorio de Estudios Cristalográficos, IACT, CSIC-Universidad de Granada, 18100 Granada, Spain; duane.choquesillo@csic.es

* Correspondence: demadis@uoc.gr



Citation: Vassaki, M.; Kotoula, C.; Turhanen, P.; Choquesillo-Lazarte, D.; Demadis, K.D. Calcium and Strontium Coordination Polymers as Controlled Delivery Systems of the Anti-Osteoporosis Drug Risedronate and the Augmenting Effect of Solubilizers. *Appl. Sci.* **2021**, *11*, 11383. <https://doi.org/10.3390/app112311383>

Academic Editors: Susana Santos Braga and Filipe Alexandre Almeida Paz

Received: 3 November 2021

Accepted: 27 November 2021

Published: 1 December 2021

Publisher's Note: MDPI stays neutral with regard to jurisdictional claims in published maps and institutional affiliations.



Copyright: © 2021 by the authors. Licensee MDPI, Basel, Switzerland. This article is an open access article distributed under the terms and conditions of the Creative Commons Attribution (CC BY) license (<https://creativecommons.org/licenses/by/4.0/>).

Abstract: Bisphosphonates (BPs) constitute a class of drugs used for the treatment of calcium- and bone-related disorders, including osteoporosis, Paget's disease, etc. The presence of the anionic phosphonate groups endows them with the ability to act as ligands to metal ions. As a result, the synthesis of complexes or coordination polymers of various structural motifs can be accomplished. In this work, the 3rd generation BP drug risedronate (RIS) was combined with biologically acceptable alkaline earth metal ions (e.g., Ca²⁺ and Sr²⁺) in an effort to synthesize new materials. These metal-RIS compounds can operate as controlled delivery systems (CDSs) when exposed to appropriate experimental conditions, such as the low pH of the human stomach. CDS networks containing Ca²⁺ or Sr²⁺ and RIS were physicochemically and structurally characterized and were evaluated for their ability to release the free RIS drug during an acid-driven hydrolysis process. Due to the low solubility of RIS at low pH, cationic additives (linear polyethyleneimine and amine-terminated polyaminoamide dendrimer) were utilized as drug solubilizers. Based on the drug release results of this study, there was an attempt to correlate the drug release efficiency with the structural features of these CDSs.

Keywords: bisphosphonate drugs; risedronate; controlled release; coordination polymers; osteoporosis

1. Introduction

Bisphosphonates (BPs) have been used as drugs for anomalies of calcium metabolism and bone disorders for over 40 years [1]. Etidronate was the first bisphosphonate drug that was synthesized, and it has been administered in humans since the late 1970s. Bisphosphonates are chemically and enzymatically stable analogues of the inorganic pyrophosphate (PPi) and they present high affinity for hydroxyapatite (HAP), the principal natural mineral component of bone and teeth. The structural stability of BPs can be realized by replacing the bridging oxygen atom in PPi with a carbon atom (Figure 1). The hydrolysis-resistant P–C–P backbone and the high affinity for bone render BPs more efficient inhibitors of bone resorption than PPi [2].

Over 300 bisphosphonates were synthesized by modifying the R₁ and R₂ substituents of the geminal (P–C–P) bisphosphonate structure. Each bisphosphonate exhibits a different binding affinity for the mineral surface and biological activity. BPs can be distinguished based on their chemical structures and their biological activities. The non-nitrogen BPs constitute the 1st generation, and they react with the aminoacyl–tRNA synthases, which integrates them with adenosine in order to form methylene-containing ATP analogues

(AppCH₂p). The cells accumulate the AppCH₂p and it later causes their apoptosis. Nevertheless, they exhibit lower efficacy as inhibitors of osteoclasts. The 2nd and 3rd generations include nitrogen-containing BPs, which present higher anti-resorptive action because they are capable to inhibit the farnesyl pyrophosphate synthase (FPPS), an important enzyme of the mevalonate pathway. As a result, they produce a toxic metabolite, which could cause osteoclast apoptosis. The 3rd generation drugs display different types of nitrogen-containing heterocyclic rings in their structures, and studies showed that they exhibit the most potent antiresorptive activity [3,4].

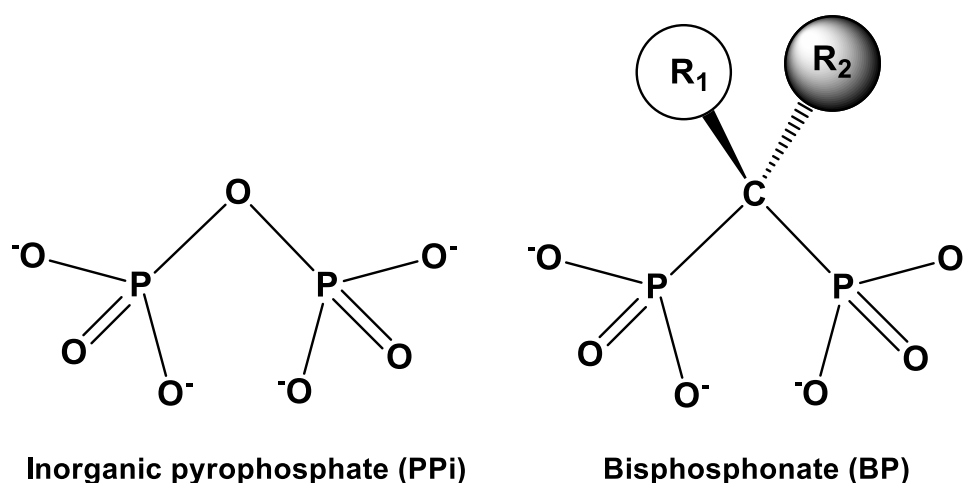


Figure 1. Schematic structures of inorganic pyrophosphate (PPI, left) and geminal bisphosphonate (BP, right), in their fully deprotonated forms.

The BP drugs are administered orally, intravenously and, in some cases, via injection. Their bioavailability is very low, with only <6% (depending on the individual BP) of the dose being absorbed by the intestine, distributed via blood in the body and finally uptaken by the bones. For that reason, the therapeutic dosages should be increased in order to achieve effective patient treatment. These high doses induce several side effects, such as hypocalcemia, osteomyelitis, osteonecrosis of the lower jaw, “flu”-like symptoms, bone pain, and gastro-intestinal, ocular and renal side effects. [5].

In order to reduce these side effects, it is necessary to devise and construct new drug delivery systems (DDSs) that could be able, ideally, to release the drug in a predictable and controlled manner. Many different types of DDS containing BP drugs have been reported. Some examples follow. Titanium implants coated with calcium zeolite were used as controlled delivery systems (CDSs) for the drug risedronate (RIS). It was found that one year is needed for the release of 30% of the total drug quantity [6]. Biphasic calcium phosphate (BCP) scaffolds were loaded with the drug alendronate (ALE). The drug release notwithstanding, the osteogenetic activity in MG-63 cells and mineralization in vivo based on a rat tibial defect model were evaluated. The drug release was dose dependent, and the ALE/BCP scaffolds operated as enhancers for bone formation [7].

Furthermore, BPs can act as organic ligands for, or linkers between, metal ions due to the presence of the anionic phosphonate groups. These display strong affinity for metal ions in aqueous solutions [8]. Metal-containing hybrid materials were constructed after the combination of BPs with biologically acceptable metal ions. Various biological applications of coordination compounds and metal organic frameworks (MOFs) have already been published [9]. Some have been evaluated for their controlled drug release features under different conditions that mimic the conditions in human body (e.g., the gastrointestinal tract). For the preparation of these compounds, metal ions, such as Ca²⁺, Mg²⁺, Zn²⁺, Fe^{2+/3+}, etc., in specific doses were utilized. Three isotypical coordination complexes with the general chemical formula $[M_2(H_4ALE)_4(H_2O)_2] \cdot 1.5H_2O$ were fabricated by the combination of the drug ALE with various amounts of Mg²⁺, Ca²⁺, or Sr²⁺ cations. The

therapeutic action of these compounds was found to be dependent on the long release period and also on the contribution of the released metal ions in order to improve the osteoblast metabolic activity [10]. Mg^{2+} - and Ca^{2+} -containing complexes and coordination polymers of various structural motifs were synthesized with four BP drugs (etidronate, pamidronate, alendronate and neridronate) [11]. They were studied as CDSs based on the premise that the metal–O(phosphonate) coordination bond can undergo hydrolysis due to the low pH, which will induce the controlled release of the active BP drug. These were coined “self-sacrificial MOFs”. The coordination of the BP drug by the metal ions resulted in substantially reduced initial release rates and lower final % release compared to the respective control system (with “free” drug and no metals). These compounds do not exhibit higher cytotoxicity than the “free” drug in the NIH3T3 mouse embryonic cell line [11].

RIS (commercial name Actonel) is a 3rd generation BP drug, which exhibits an affinity constant $K_{app} = 21.9 \pm 1.7 \times 10^5 M^{-1}$ for hydroxyapatite. This value is higher than those of the 2nd generation BPs, but lower than those of the other 3rd generation BPs [12]. The binding affinity influences drug absorption and retention by the bone skeleton, the release of the absorbed drug and also the half-life of its attachment on the bone surface. These features affect its osteoclast inhibition potency. RIS was approved in 1998 for the treatment of several bone-related disorders (e.g., postmenopausal, corticosteroid-induced osteoporosis).

Recently, we initiated a systematic multi-approach study of metal-containing coordination polymers in which the linker is a BP drug. The scope of this study includes the reliable and reproducible synthesis of such metal–BP systems, their full structural elucidation, and, most importantly, their ability to act as “self-sacrificial” sources of the BP drug. In this work, the 3rd generation anti-osteoporotic drug RIS was used for the synthesis of two new coordination polymers, namely $[Ca(RIS)(H_2O)]_n$ (Ca–RIS) and $[Sr(RIS)(H_2O)]_n$ (Sr–RIS). These two novel compounds were physicochemically and structurally characterized and were also evaluated for their RIS release features under acidic conditions (pH = 1.3) that mimic the human stomach. Importantly, it was observed that RIS shows low solubility under acidic conditions. Hence, in order to fully and reliably study the drug release profiles of “free” RIS, Ca–RIS and Sr–RIS, it was necessary to utilize two cationic drug solubility enhancers, namely, a linear polyethyleneimine polymer (LPEI) and an amine-terminated polyaminoamide dendrimer (PAMAM-2). To the best of our knowledge, this is the first systematic controlled release study of the RIS drug.

2. Materials and Methods

2.1. Instrumentation

Scanning electron microscopy. Elemental analyses and SEM images of the morphology of the metal–BPs collected with a JOEL JSM-6390LV electron microscope.

Single crystal X-ray diffraction. Measured crystals were prepared under inert conditions immersed in perfluoropolyether as protecting oil for manipulation. Suitable crystals were mounted on MiTeGen Micromounts™, and these samples were used for data collection. Data for Ca–RIS and Sr–RIS were collected with a Bruker D8 Venture diffractometer with graphite monochromated $CuK\alpha$ ($\lambda = 1.54178 \text{ \AA}$, for Ca–RIS) or $AgK\alpha$ ($\lambda = 0.56086 \text{ \AA}$, for Sr–RIS). The data were processed with APEX3 suite [13]. The structures were solved by intrinsic phasing using the ShelXT program [14], which revealed the position of all non-hydrogen atoms. These atoms were refined on F^2 by a full-matrix least-squares procedure, using the anisotropic displacement parameter [15]. All hydrogen atoms were located in difference Fourier maps and included as fixed contributions riding on attached atoms with isotropic thermal displacement parameters 1.2- or 1.5-times those of the respective atom. The Olex2 software was used as a graphical interface [16]. Molecular graphics were generated using mercury [17]. The crystallographic data for the reported structure was deposited with the Cambridge Crystallographic Data Center as supplementary publication

nos. CCDC 2118543 and 2118546. Copies of the data can be obtained free of charge at <http://www.ccdc.cam.ac.uk/products/csd/request>.

Powder X-ray diffraction. The powder X-ray diffraction (XRD) patterns were performed on PANalytical X'Pert Pro diffractometer, a configuration of the Bragg–Brentano, equipped with monochromator Ge(111) (Cu $K_{\alpha 1}$) and detector X'Celerator.

Hydrothermal high-throughput synthesis setup. The hydrothermal syntheses of metal–BPs were conducted in a laboratory oven, in a custom-made autoclave system composed of 36 Teflon-lined reaction chambers (volume 5 mL). The syntheses were carried out under autogenous pressure in parallel. The chambers were covered by a thin Teflon sheet, which was enclosed inside the aluminum autoclave, in order to avoid any solvent leaks.

2.2. Materials

All reagents that were utilized as sources of metal ions were from commercial sources. Strontium chloride hexahydrate ($\text{SrCl}_2 \cdot 6\text{H}_2\text{O}$) and calcium chloride dihydrate, ($\text{CaCl}_2 \cdot 2\text{H}_2\text{O}$) were purchased from Sigma-Aldrich (St. Louis, MO, USA). The dendrimer PAMAM-2 (42% *w/w* methanol solution) was a gift from Dendritech Inc. (Midland, MI, USA). Linear polyethyleneimine (LPEI, MW 22,000 Daltons) was obtained from Polysciences, Inc. (Warrington, PA, USA). The tablet excipients lactose (Serva), cellulose (Merck) and silica (Alfa-Aesar) were from commercial sources.

2.3. Synthetic Protocols

Synthesis of sodium hydrogen (1-hydroxy-1-phosphono-2-(pyridin-3-yl)ethyl) phosphonate (sodium risedronate pentahemihydrate, Na-RIS-2.5H₂O). The sodium salt of RIS was prepared by following a previously reported methodology, but with some modifications [18]. A mixture of 3-pyridineacetic acid hydrochloride (30 g, 0.17 mol), phosphorous acid (14.2 g, 0.17 mol), and methanesulfonic acid (60 mL) was heated to 65–70 °C followed by the addition of PCl_3 (30.2 mL, 47.5 g, 0.35 mol, 2.0 eq) for over 0.5–1 h under nitrogen atmosphere. After the PCl_3 addition, the mixture was stirred overnight at 65–70 °C, and cold distilled water (200 mL) was added to a cooled solution with vigorous stirring. After refluxing overnight, the reaction mixture was allowed to cool to room temperature and pH adjusted to 4–4.5 by 50% NaOH. Then, 200 mL of EtOH was added by stirring and the mixture was left overnight at ambient temperature. The formed solid was collected by filtration, washed with 50% EtOH and finally with acetone, and dried under reduced pressure. The final product (Na-RIS-2.5H₂O) was obtained as a white powder (45.5 g, 86% yield). ¹H NMR (D₂O): δ 8.75–8.72 (m, 1H), 8.59–8.55 (m, 2H), 7.94–7.90 (m, 1H), 3.45 (t, 2H, ³J_{HP} = 12.1). ¹³C NMR (D₂O, CD₃OD as ref.) δ 150.1, 143.3, 139.4, 139.1 (t, ³J_{CP} = 9.0), 126.9, 74.5 (t, ¹J_{CP} = 134.2, P-C-P), 37.0. ³¹P NMR (D₂O) δ 17.0.

Hydrothermal synthesis of Ca–RIS. Na-RIS-2.5H₂O (9 mg, 0.025 mmol) and $\text{CaCl}_2 \cdot 2\text{H}_2\text{O}$ (2 mg, 0.0125 mmol) were dissolved in 3.25 mL H₂O. The solution pH was adjusted to 2.5 (using stock solutions of NaOH and HCl, as needed). The final mixture was placed in a Teflon-lined reactor and was heated at 120 °C for 3 days. After cooling at room temperature, colorless crystals formed and were isolated by filtration. Bulk product purity was confirmed by powder X-ray diffraction (comparison of the calculated and experimental powder patterns) and elemental analyses. Yield: 2 mg (47%). The synthesis of Ca–RIS was also repeated at a Ca:RIS molar ratio of 1:1. The same product was obtained, albeit at lower yields (26%). Elemental analysis: Calcd. for $\{\text{Ca}[(\text{C}_5\text{H}_4\text{NH})\text{CH}_2\text{C}(\text{OH})(\text{PO}_3\text{H})(\text{PO}_3)](\text{H}_2\text{O})\}_n$, M.W. 339.19: C 24.79; H 3.27; N 4.13. Found: C 24.94; H 3.40; N 4.10.

Hydrothermal synthesis of Sr–RIS. Na-RIS-2.5H₂O (35 mg, 0.10 mmol) and $\text{SrCl}_2 \cdot 6\text{H}_2\text{O}$ (13 mg, 0.05 mmol) were dissolved in 3.25 mL H₂O. The solution pH was adjusted to 2.5 (using stock solutions of NaOH and HCl, as needed). The final solution was placed in a Teflon-lined reactor and was heated at 120 °C for 3 days. After cooling at room temperature, colorless crystals formed and were isolated by filtration. Bulk product purity was

confirmed by powder X-ray diffraction (comparison of the calculated and experimental patterns) and elemental analyses. Yield: 4 mg (21%). The synthesis of Sr-RIS was also repeated at a Sr:RIS molar ratio of 1:1. The same product was obtained, albeit at lower yields (5%). Elemental analysis: Calcd. for $\{Sr[(C_5H_4NH)CH_2C(OH)(PO_3H)(PO_3)](H_2O)\}_n$, M.W. 386.73: C 21.74; H 2.87; N 3.62. Found: C 21.73; H 2.96; N 3.54.

Scaled-up synthesis of Ca-RIS. Na-RIS·2.5H₂O (175 mg, 0.50 mmol) was dissolved in 65 mL H₂O, and the pH of the solution was adjusted to 2.5 (using stock solution of HCl, as needed). Subsequently, CaCl₂·2H₂O (73 mg, 0.50 mmol) was added to that solution under stirring. The final mixture was placed in a flask and heated at 80 °C under stirring for 3 days. A white microcrystalline powder precipitated, which was isolated by filtration and washed with deionized water. Product purity was confirmed by powder X-ray diffraction (comparison of the calculated and experimental patterns of Ca-RIS). Yield: 65 mg (38%).

2.4. Preparation of Tablets for Drug Release

Tablets were prepared by mechanical mixing of ground powders (with a mortar-and-pestle) of the drug component (850 µmol of RIS content) and three commonly used excipients, i.e., lactose, cellulose and silica. Subsequently, a tablet was produced by applying 10 tons of pressure in a hydraulic press. The tablet total weight was 1.000 g. Identical tablets were fabricated that contained equimolar amounts of the metal-BPs (Ca-RIS and Sr-RIS) and the three excipients. The quantities used in tablets are shown in Table 1.

Table 1. Quantities of active agents (free drug or metal-BPs) and excipients utilized for tablet preparation.

Tablet	Na-RIS·2.5H ₂ O	Ca-RIS	Sr-RIS
MW (g/mol)	350.13	339.19	386.73
Drug mass (g)	0.298	0.288	0.329
Lactose (g)	0.234	0.237	0.224
Cellulose (g)	0.234	0.237	0.224
Silica (g)	0.234	0.237	0.224

2.5. Quantification of Drug Controlled Release

Each tablet described above was immersed in a glass beaker containing 50 mL of deionized water whose pH was adjusted to 1.3, using hydrochloric acid. The RIS-containing tablet (as prepared above) was placed in a plastic net and was immersed into the solution (50 mL of deionized water whose pH was adjusted to 1.3 using hydrochloric acid) just above the stirring bar. Mild stirring was applied to ensure solution homogeneity. The solution was sampled (sample volume 350 µL) every hour for the first 6 h, and every 3 h until the 12th hour, and every 12 h until the 48th hour of the release experiment. After the 48th hour, samples were withdrawn every 24 h or every 48 h or longer, if necessary. Each sample was placed in an NMR tube, and then the D₂O standard solution (150 µL) was added. The concentration of the D₂O TSP standard solution was 4.337 µmol. Quantification of RIS concentration in each sample was achieved by peak integration (singlet at 8.7 ppm, which is the H on the C between the pyridine N and the C next to the methylene group) in the ¹H NMR spectrum and its comparison to the peak of the TSP standard solution peak [-Si(CH₃)₃].

2.6. Quantification of Drug Controlled Release in the Presence of PAMAM-2 Dendrimer

The “free” RIS-containing tablet was immersed in a glass beaker consisting of 48 mL of deionized water and PAMAM-2 dendrimer (236.5 µmol, 2 mL of a ~42% w/w methanol solution). The RIS:PAMAM-2 molar ratio was 3.5:1 (1 RIS molecule per 4.5 surface amine groups). The final pH of the solution was adjusted to 1.3, using hydrochloric acid. The bulk solution was placed under mild stirring homogeneity. The sampling protocol was the same as the one described in the previous section.

2.7. Quantification of Drug Controlled Release in the Presence of LPEI

Solid LPEI polymer (435 mg, 850 μmol) was dissolved in a glass beaker containing 50 mL of deionized water. The pH of the solution was adjusted to 1.3 using hydrochloric acid. The “free” RIS-containing tablet was immersed into the solution. The RIS:LPEI molar ratio was 1:1 (1 RIS molecule per 1 polymer unit). The bulk solution was placed under mild stirring homogeneity. The sampling protocol was the same as the one described in the previous section.

3. Results

3.1. Synthesis and Characterization of (Ca/Sr)–RIS Compounds

The new (Ca/Sr)–RIS compounds were synthesized under hydrothermal conditions in water, by reacting Na-RIS·2.5H₂O with calcium and strontium chloride, respectively, at pH 2.5. The solution pH is crucial for isolating tractable products. Excessively low pH will cause crystallization of unreacted RIS (Na-RIS·2.5H₂O), whereas high pH will result in fast product precipitation that is usually amorphous, or with low crystallinity. Inevitably, extensive experimentation with various solution pH values must be carried out. It was found that the pH of 2.5 is optimal for the isolation of a pure, monophasic product. The hydrothermal syntheses yielded single crystals suitable for X-ray diffraction studies. The crystals were isolated and studied by scanning electron microscopy. The crystal morphology of the two compounds is shown in Figure 2.

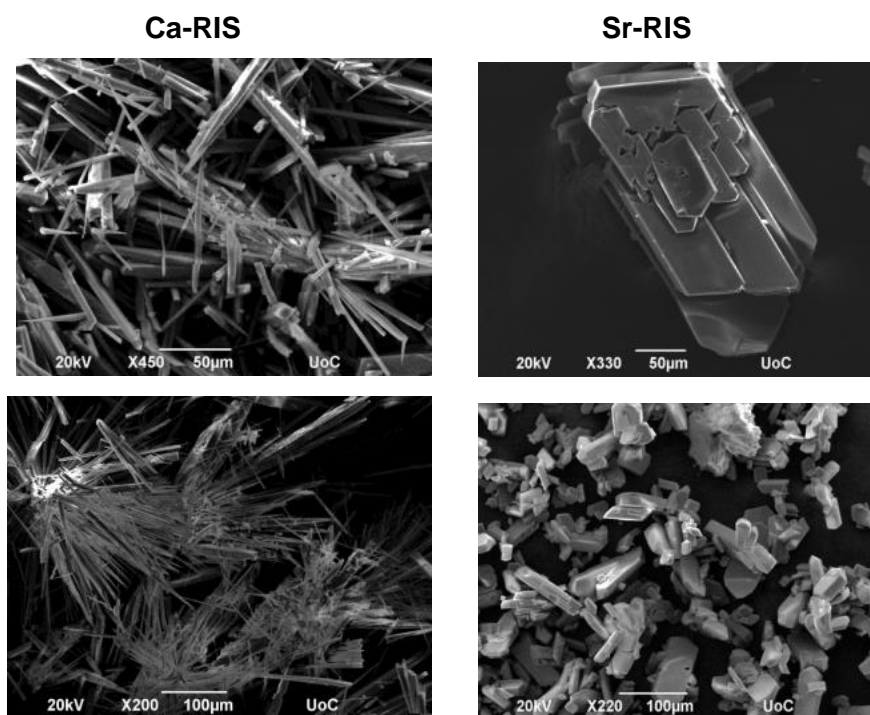


Figure 2. SEM images of single crystals of metal-BPs.

3.2. Powder and Single Crystal X-ray Diffraction Studies of (Ca/Sr)–RIS Compounds

Bulk solid products of the (Ca/Sr)–RIS compounds were studied by powder X-ray diffraction to ensure that they were pure and monophasic. Comparison of the calculated (from the crystal structure determination, see below) and measured X-ray diffraction diagrams, ensured that the samples were pure (Figure 3).

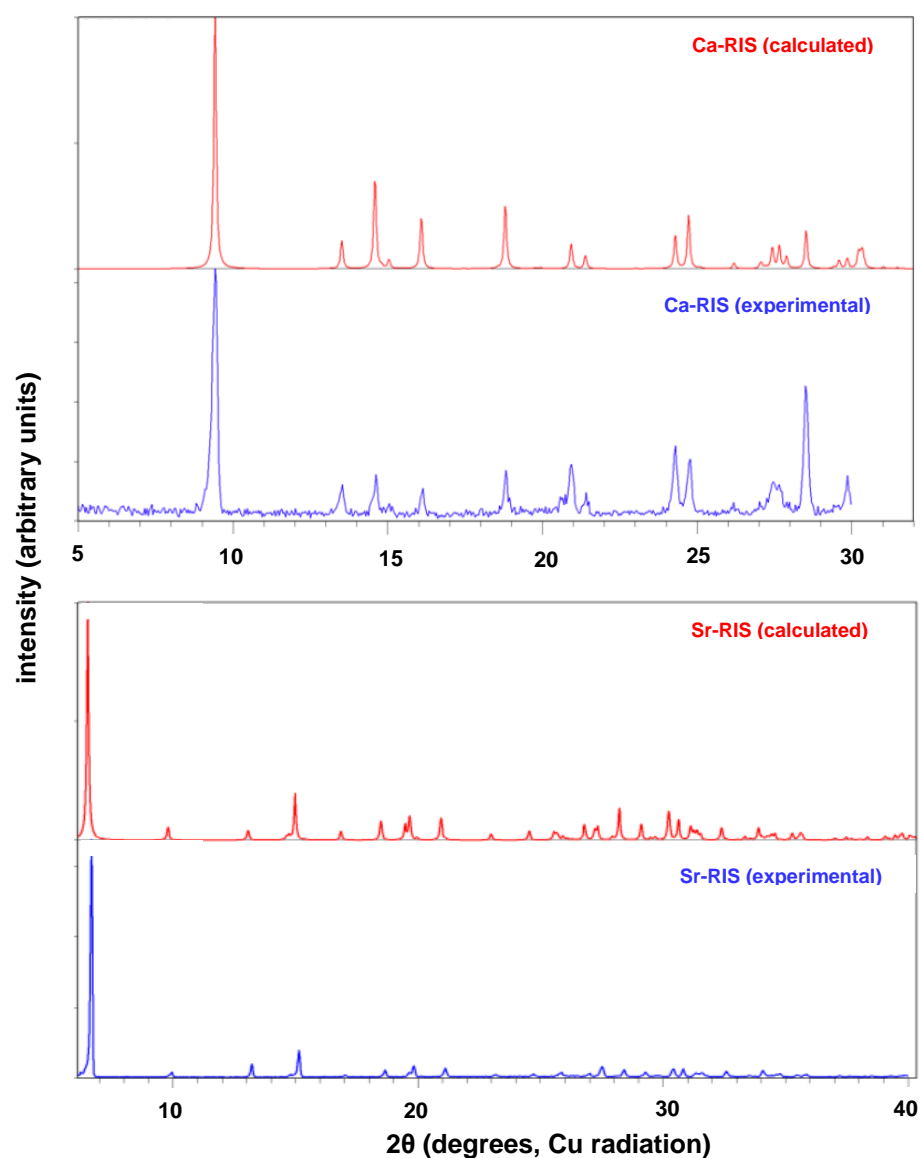


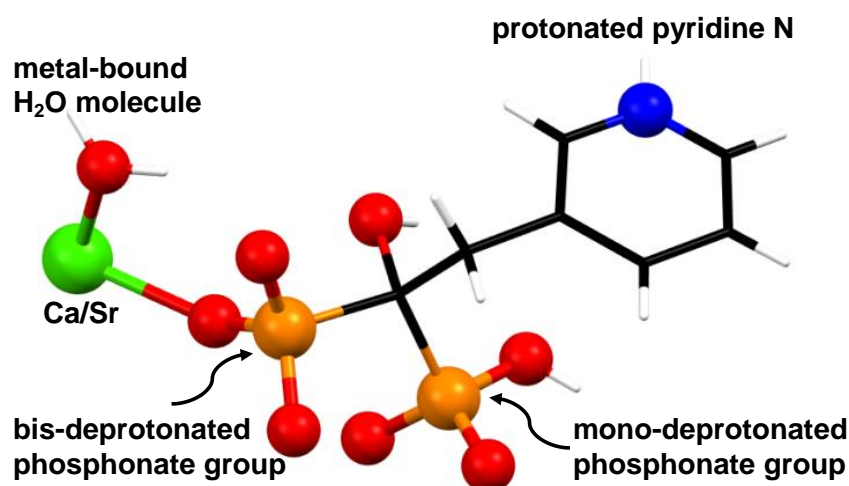
Figure 3. Calculated (red) and measured (blue) powder X-ray diffraction diagrams of Ca-RIS (**upper**) and Sr-RIS (**lower**).

Suitable crystals for single crystal X-ray diffraction and structure determination were obtained by hydrothermal syntheses (see above). The crystallographic data of the compounds Ca-RIS and Sr-RIS are summarized in Table 2 and their cif files are provided as Supplementary Materials.

The RIS ligand exhibits a total charge of “−2” to counterbalance the “+2” charge of the metal cation in both structures of Ca and Sr-RIS. This means that one of the phosphonate groups (P2) is mono-deprotonated, whereas the other (P1) is bis-deprotonated. The N of the pyridine ring is protonated. Hence, RIS behaves as a zwitterion in the structure. The asymmetric unit of the two compounds Ca- and Sr-RIS is shown in Figure 4.

Table 2. Crystal data for compounds Ca–RIS and Sr–RIS.

	Ca–RIS	Sr–RIS
Empirical formula	C ₇ H ₁₁ CaNO ₈ P ₂	C ₇ H ₁₁ SrNO ₈ P ₂
<i>M_r</i>	339.19	386.73
Crystal system	orthorhombic	monoclinic
Space group	P2 ₁ 2 ₁ 2 ₁	P2 ₁ /n
a (Å)	6.7990(9)	13.679(5)
b (Å)	13.091(2)	12.101(3)
c (Å)	13.446(2)	6.987(4)
α (°)	90	90
β (°)	90	98.170(15)
γ (°)	90	90
V (Å³)	1196.77	1144.82
Z	4	4
R factor (%)	5.71	3.19
CCDC code	2118543	2118546

**Figure 4.** Asymmetric unit of Ca- and Sr–RIS. Color codes: metal centers, green; P, orange; O, red; C, black; N, blue; H, white.

In compound Ca–RIS, the coordination sphere of the Ca²⁺ center can be described as a pentagonal bipyramid (*D*_{5h}, based on SHAPE analysis), while it forms six coordination bonds with oxygen atoms of three different RIS ligands and one bond with a water molecule. Each RIS ligand coordinates to three metals, and hence, Ca–RIS is a 1D coordination polymer. The Ca²⁺ cation chains are arranged in such a way that they lie parallel to the *a*-axis (Figure 5a). The Ca–O bond distances (Figure 5b) are between 2.292 Å and 2.633 Å. There are H bonds between the chains: one O(phosphonate)⋯O(P-hydroxy) interaction [2.454 Å], one O(hydroxy)⋯O (water) interaction [2.743 Å], one O(phosphonate)⋯O(water) interaction [2.827 Å] and one N(1)⋯O(phosphonate) [2.652 Å].

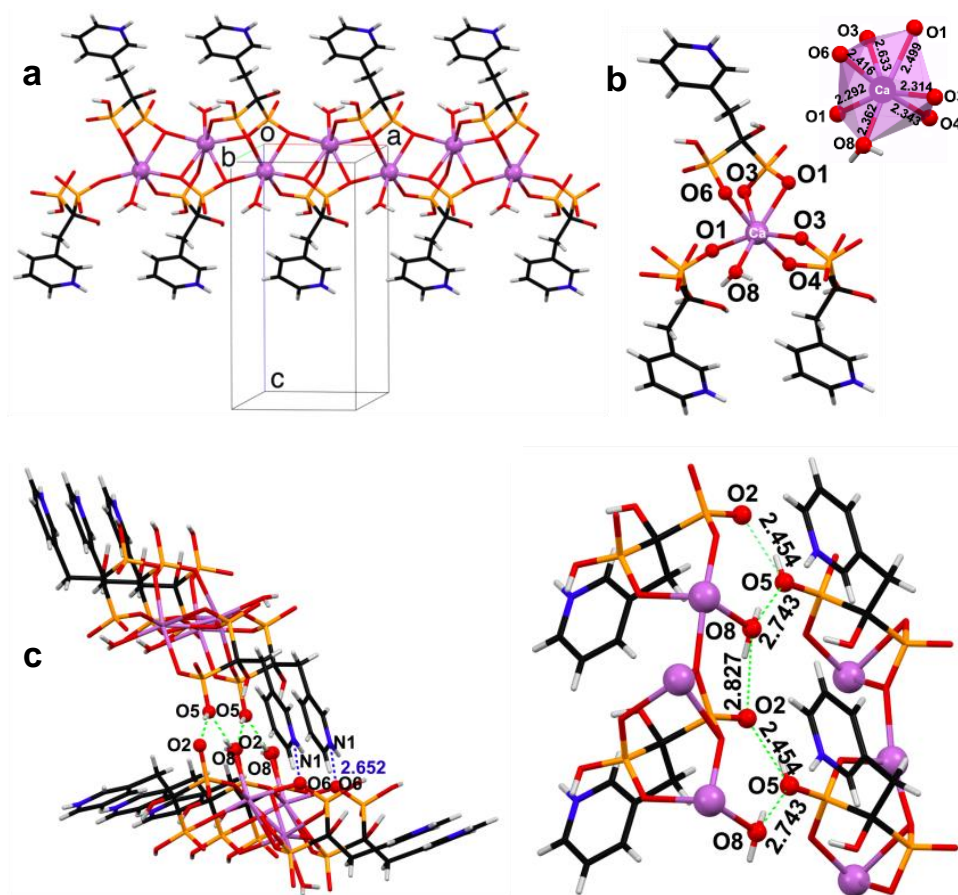


Figure 5. Various views of the crystal structure of Ca-RIS: (a) a single 1D chain along the a-axis, (b) the coordination sphere of the of Ca^{2+} center with Ca–O bond distances, and (c) the hydrogen bonding schemes (dashed green lines) between the 1D chains. Color codes: Ca, purple; P, orange; O, red; C, black; N, blue; H, white.

Compound Sr-RIS is a 2D coordination polymer. Its layers are constructed along the b- and c-axes (Figure 6a). Each Sr^{2+} center is coordinated by four different RIS ligands through seven oxygen atoms and is also coordinated by a water molecule. The geometry of Sr1 in compound (II) is a biaugmented trigonal prism (C_{2v} , based on SHAPE analysis, Figure 6c). The structure does not display any inter-layer H bonds, but there are some intra-layer H bonds, as well as “ π - π ” stacking interactions between the pyridyl rings (Figure 6b).

3.3. Controlled Release Study of “Free” RIS, Ca-RIS and Sr-RIS

Three controlled delivery systems (CDSs) were evaluated in the form of tablets: (a) the “free” drug risedronate, (b) Ca-RIS, and (c) Sr-RIS. The active agents, the “free” RIS drug and its metal-RIS coordination compounds were mixed and ground with the appropriate excipients in the solid form, and these powders were pressed into tablets. These tablets were immersed into acidic solutions and aliquots were withdrawn at specific time intervals. The detailed protocols for tablet preparation, sampling and drug quantification are described in detail in Sections 2.4 and 2.5. Under the acidic conditions of the drug release experiments, hydrolysis of the metal–O bonds occurs that leads to the degradation of the crystal lattice and the release of RIS into the acidic medium. The drug release was quantified by ^1H NMR spectroscopy and the results were plotted in graphs as “% drug” vs. time (in hours).

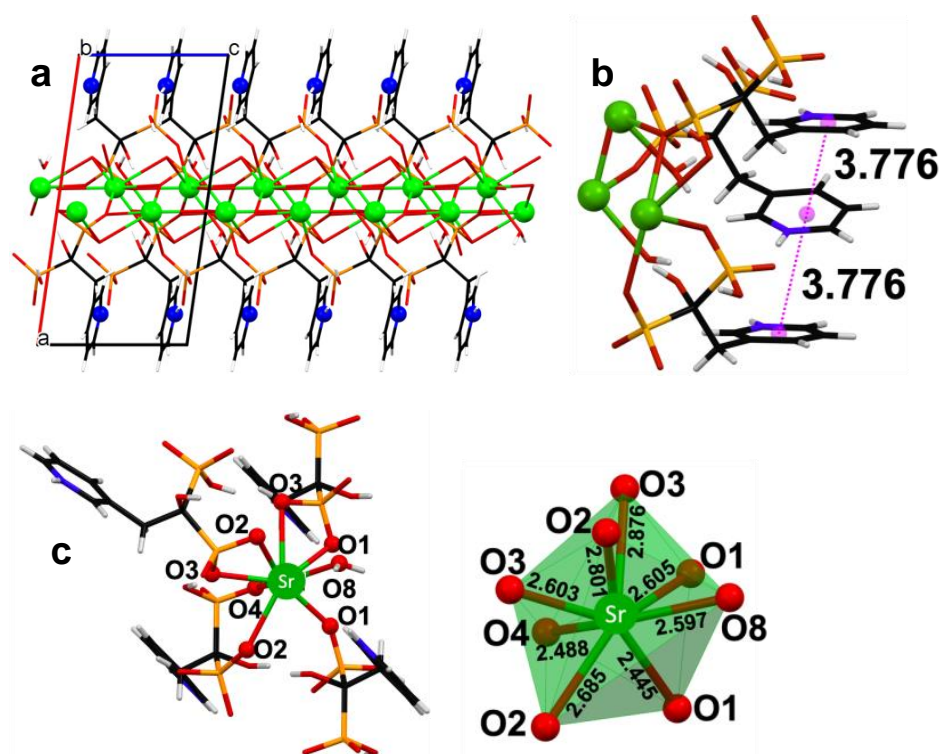


Figure 6. Various views of the crystal structure of Sr-RIS: (a) view of 2D layers (hydrogen atoms are omitted for clarity), (b) “ π - π ” stacking interactions between the pyridyl rings, and (c) the coordination sphere of the of Sr^{2+} center with Sr-O bond distances. Color codes: Sr, green; P, orange; O, red; C, black; N, blue; H, white.

With tablets containing the “free” RIS drug (with excipients), a fast release was observed during the first 2 h of the experiments, followed by a gradual drop in the quantity of RIS in solution (Figure 7). Crystal formation was noted. The experiment was stopped after 72 h; the clear colorless crystals were collected by filtration and were analyzed by powder X-ray diffraction. It was unequivocally proven that the precipitated solid was risedronic acid monohydrate, which is sparingly soluble in acidic solutions (inset of Figure 6) [19]. The gradual drop on measured “free” RIS is undoubtedly due to the low solubility of risedronic acid monohydrate (at the experimental pH). This is evidenced by the complicated H-bonding network of the phosphonate and pyridinium groups and the lattice water molecule, and by the strong π - π interactions between the pyridyl rings (centroid-to-centroid 3.485 Å) of neighboring RIS molecules.

The insolubility of the risedronic acid under these acidic conditions hampered the implementation of reliable release experiments and prohibited any meaningful comparisons with the release profiles of the Ca/Sr-RIS systems. Therefore, appropriate cationic additives were sought that could act as drug solubilizers. This strategy was based on the notion that the additive’s cationic groups will form electrostatic interactions with the anionic phosphonate groups of the RIS drug, thus preventing its crystallization. Two cationic additives were tested, namely, an amine-terminated polyamidoamine dendrimer (PAMAM of generation 2 with 16 surface $-\text{NH}_2$ groups) and a linear polyethyleneimine polymer (LPEI, of MW 22,000 Daltons). Their schematic structures are shown in Figure 8. These additives were used in our group for the stabilization of anionic silicate in aqueous systems [20–25].

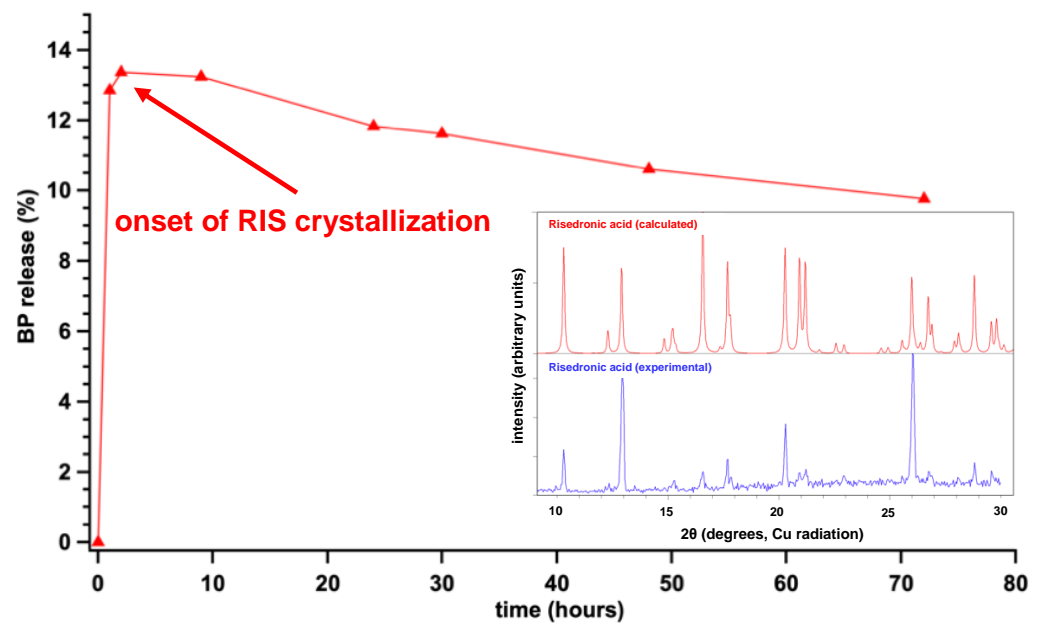


Figure 7. Controlled release of “free” RIS, showing the onset of its crystallization in acidic solution. Inset: calculated (red) and measured (blue) powder X-ray diffractograms (calculated and measured) of RIS acid.

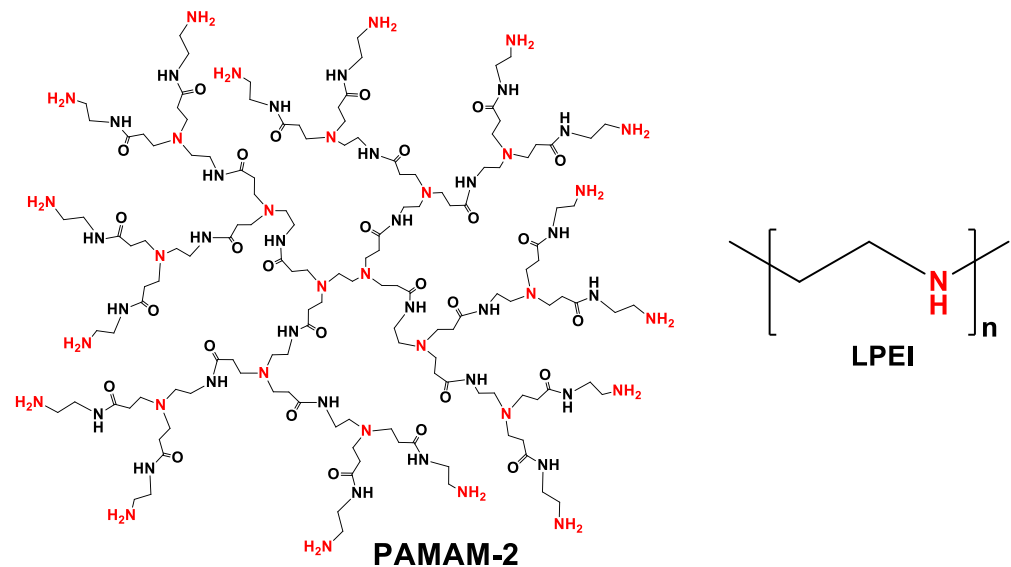


Figure 8. Schematic structures of PAMAM-2 and LPEI, used as solubility enhancers of RIS. The amine groups that are protonated in acidic solutions are highlighted red.

LPEI was used in such a quantity that the RIS:amine molar ratio was 1:1. PAMAM-2 was added in excess, so the RIS:amine(surface) molar ratio was 1:4.5. Two different experiments were conducted. Initially, the PAMAM-2 and LPEI additives were tested as drug solubilizers for the “free” RIS system in a “proof-of-concept” experiment. The results are depicted in Figure 9 and demonstrate the efficacy of the additives to prevent the precipitation of RIS acid monohydrate. No drop in RIS concentration was observed, and the release profiles were as expected, showing a rise in drug concentration during the first hours that eventually led to a plateau. The release of RIS in the presence of PAMAM-2 showed an initial rate of 0.08 $\mu\text{mol}/\text{min}$, reaching a plateau at $\sim 5\%$ after 10 h. The release of RIS in the presence of LPEI was slightly faster, and showed an initial rate of 0.10 $\mu\text{mol}/\text{min}$, reaching a plateau at $\sim 35\%$ after 250 h. Since LPEI was proven to be a more effective RIS

solubilizer, the next experiments were focused on using this additive for the evaluation of the metal-containing systems.

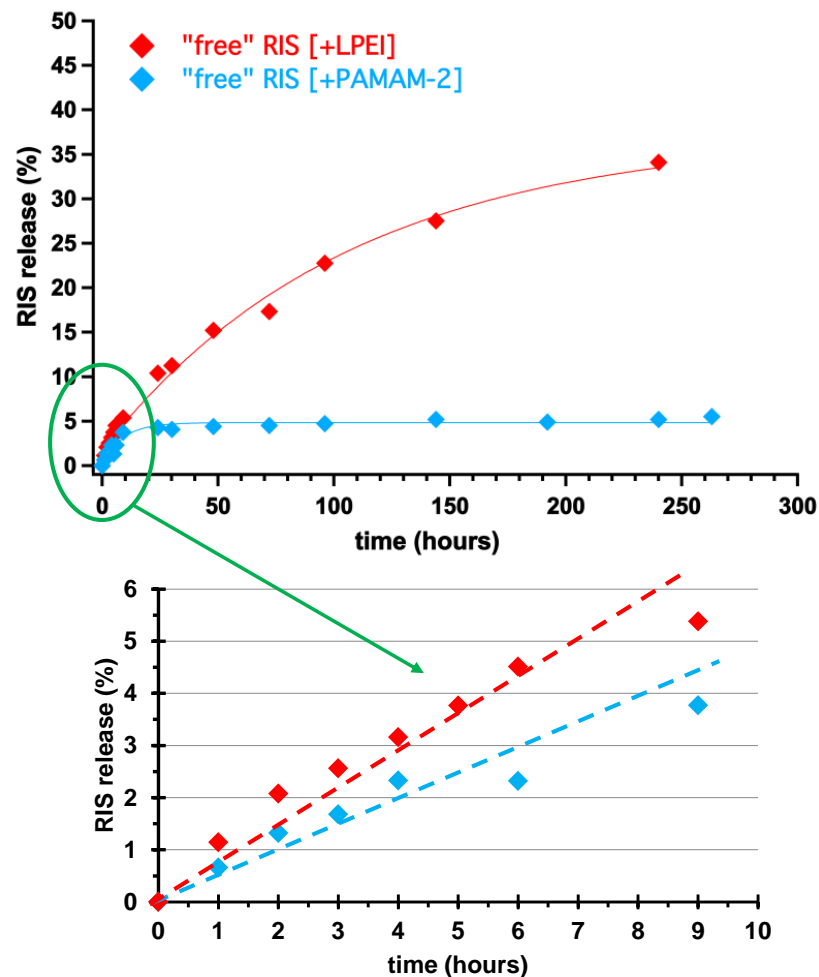


Figure 9. Controlled release of "free" RIS in the presence of cationic additives, LPEI (red) and PAMAM-2 (light blue) at pH = 1.3. **Upper:** long-term RIS release. **Lower:** initial stages of RIS release.

After proving the beneficial effects of the cationic additives as drug solubilizers, experiments were set up, using Ca- and Sr-RIS as the CDSs in the presence of LPEI. The release curves are shown in Figure 10. In contrast to other metal-containing BP systems [11], these experiments revealed that the metal-containing tablets exhibited faster RIS release than those containing the "free" drug (no metals). Specifically, the initial rate observed for Ca-RIS was $0.44 \mu\text{mol}/\text{min}$, and for Sr-RIS, it was $0.52 \mu\text{mol}/\text{min}$. These initial rate values can be compared to that for the "free" RIS system, $0.10 \mu\text{mol}/\text{min}$. The final % release values were also higher for the Ca-RIS (~75%) and the Sr-RIS (~60%) systems, compared to the "free" RIS system (~35%). An explanation for the difference in the plateau values in the Ca- and Sr-RIS CDSs is not immediately obvious. Based on these and previous results [11], it seems to be dependent on the metal cation and the released drug itself since all other variables (pH, geometrical features of the tablet, and amount of active drug) are the same. Apparently, further experimentation is needed to delineate this point. Interpretation of these results is presented in the following discussion section.

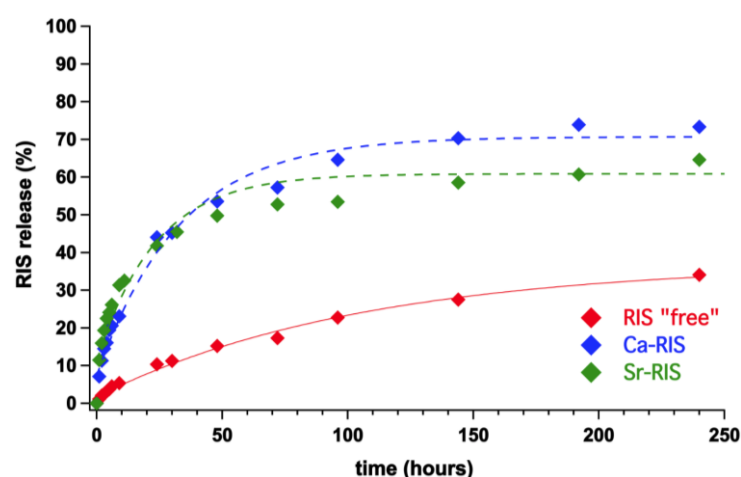


Figure 10. RIS release curves from Ca- and Sr-RIS containing tablets and comparison with the “free” RIS system. The experiments were performed in the presence of LPEI at pH = 1.3.

4. Discussion

The published crystal structures containing the BP risedronate include its “free” forms and its metal-containing forms. The “free” forms include risedronic acid monohydrate [19,26], the dihydrate [27], and the ammonium dihydrate [27]. The RIS derivatives that incorporate some kind of metal ion include the Na dihydrate and 2.5 hydrate [19], the K dihydrate [27], the Mg, Ni, and Fe coordination polymer derivatives [28], the Cu and Ni molecular complex derivatives [29] and a Cd coordination polymer [30]. With this paper, two more metal derivatives of RIS are added to the above list: the Ca- and Sr-RIS compounds. In this section, we discuss the behavior of the Ca- and Sr-RIS systems as controlled release agents.

The controlled release curves of all systems studied here are shown in Figures 9 and 10. As shown above, the utilization of cationic organic additives (PAMAM-2 dendrimer and LPEI polymer) was necessary to avoid bulk crystallization of the released RIS into the acidic medium. The results obtained here show that the metal-containing RIS systems exhibit higher initial release rates than the “free” RIS system (no metals). This observation is in contrast to what was observed before in our previous work [11] for other BP drugs, in which the “free” drug was released much faster than the metal-containing drugs. The results obtained herein appear to be counterintuitive because the “free” RIS is released much more slowly than in the Ca-RIS and Sr-RIS systems. The latter systems need to overcome the acid hydrolysis of the metal–O bond in order to release RIS. In this section, we attempt to interpret the drug release results based on the various interactions noted in the solid state of RIS monohydrate, Ca-RIS and Sr-RIS.

The slow initial rate for the “free” RIS may be related to the stability of the crystal lattice of the compound. The water solvent must overcome several stabilizing interactions. There are strong π – π interactions between the pyridyl rings (centroid-to-centroid distance 3.487 Å). These are hydrophobic interactions, so the solvent (water) cannot penetrate the crystal lattice and “break” them. The presence of one lattice water further stabilizes the crystal structure because hydrogen bonds are formed with the phosphonate groups. The phosphonate groups of RIS form nine hydrogen bonds overall.

The Ca-RIS compound can be described as a 1D coordination polymer, propagated by Ca–O(phosphonate) bridging. There are weak π – π interactions between the RIS pyridyl rings since the centroid-to-centroid distance is very long (5.340 Å). There are three H-bonding interactions (per molecular unit) between the chains (Figure 5b,c). This means that the chains can be easily penetrated by the water solvent and the Ca–O bonds can be effectively hydrolyzed in the acidic medium.

The Sr-RIS compound is a 2D coordination polymer. This compound presents the fastest initial rate. Careful examination of its crystal structure reveals that the layers are

not stabilized by H bonding, and for that reason, they can be readily exfoliated by the water solvent. Thus, the Sr–O bonds are exposed to the acidic medium and could be easily hydrolyzed. Nevertheless, there are π – π interactions between the RIS pyridyl rings (centroid-to-centroid distance 3.837 Å) (Figure 6b), but based on the centroid-to-centroid distance, they are weaker than those in the structure of “free” RIS. It is interesting that the pyridyl rings are not exactly parallel to each other, and this “tilting” may further weaken these interactions.

The Ca–RIS system displayed a somewhat slower RIS release than the Sr–RIS system (0.44 $\mu\text{mol}/\text{min}$ vs. 0.52 $\mu\text{mol}/\text{min}$). The Ca–O bond distances are shorter (average 2.416 Å) than the Sr–O bond distances (average 2.643 Å). According to HSAB (hard–soft acid–base) theory, the Ca^{2+} cations form stronger bonds with oxygen atoms than the Sr^{2+} cations. This could be a plausible explanation for the higher resistance of the Ca–O bonds towards hydrolysis, and as a result, the RIS drug is released at a much slower rate.

5. Conclusions

The main findings of the present study are as follows:

- (1) Two novel coordination polymers containing the alkaline-earth metal ions Ca^{2+} and Sr^{2+} and the anti-osteoporotic drug RIS were synthesized and structurally characterized.
- (2) Ca–RIS is a 1D coordination polymer, whereas Sr–RIS is a 2D layered coordination polymer.
- (3) Both Ca- and Sr–RIS were utilized as controlled release systems (excipient-containing tablets) of the active drug RIS in conditions that mimic the human stomach (pH = 1.2). Because RIS is a sparingly-soluble drug in acidic solutions, it was necessary to use drug solubilizers. The ones tested were the PAMAM-2 amine-terminated cationic dendrimer and the LPEI cationic polymer. Both effected smooth RIS release and prevented its precipitation.
- (4) The drug release profiles Ca- and Sr–RIS (in the presence of LPEI) were compared to that of “free” RIS (absence of metals), and it was found that they release RIS 4–5 times faster than the “free” RIS system.
- (5) This behavior was rationalized based on the structural idiosyncrasies of each system. The overall drug release profile for each system was the result of several structural factors, such as presence or absence of π – π interactions between the RIS pyridyl rings, H-bonding interactions and strength of the metal–O(phosphonate) bonds.

Based on these results, the utility of cationic solubility enhancers is highlighted, which could find application in other poorly-soluble, anionically charged drugs. Finally, the role of the metal cation in such coordination polymers apparently influences both the initial drug release rates and the final plateau release value. Hence, with proper selection of the metal ion, these features can be controlled.

Further studies are underway in our laboratory that include different types of drug hosts (e.g., hydrogels [31,32]) and the mapping of several other anti-osteoporotic drugs with a variety of structural features.

Supplementary Materials: The following are available online at <https://www.mdpi.com/article/10.3390/app112311383/s1>, cif files for Ca–RIS and Sr–RIS compounds.

Author Contributions: Conceptualization, K.D.D.; methodology, M.V., P.T. and C.K.; investigation, M.V., P.T. and C.K.; data curation, M.V., P.T. and C.K.; writing—original draft preparation, M.V.; writing—review and editing, K.D.D., M.V., C.K., P.T. and D.C.-L.; supervision, K.D.D., project administration, K.D.D., funding acquisition, M.V. and K.D.D. All authors have read and agreed to the published version of the manuscript.

Funding: The research work at UoC was supported by the Hellenic Foundation for Research and Innovation (HFRI) under the HFRI PhD Fellowship grant (Fellowship Number: 258) to M.V.D. Ch.-L. acknowledges funding by project no. PGC2018-102047-B-I00 (MCIU/AEI/FEDER, UE).

Institutional Review Board Statement: No animals were involved in this research.

Informed Consent Statement: No humans were involved in this research.

Data Availability Statement: Available upon request from the corresponding author.

Conflicts of Interest: The authors declare no conflict of interest.

References

1. Xu, X.-L.; Gou, W.-L.; Wang, A.-Y.; Wang, Y.; Guo, Q.-Y.; Lu, Q.; Lu, S.-B.; Peng, J. Basic research and clinical applications of bisphosphonates in bone disease: What have we learned over the last 40 years? *J. Transl. Med.* **2013**, *11*, 303. [[CrossRef](#)] [[PubMed](#)]
2. Russell, R.G. Bisphosphonates: From bench to bedside. *Ann. N. Y. Acad. Sci.* **2006**, *1068*, 367–401. [[CrossRef](#)] [[PubMed](#)]
3. Barbarosa, J.S.; Paz, F.A.A.; Braga, S.S. Bisphosphonates, Old Friends of Bones and New Trends in Clinics. *J. Med. Chem.* **2021**, *64*, 1260–1282. [[CrossRef](#)] [[PubMed](#)]
4. Bartl, R.; Frisch, B.; Tresckow, E.; Bartl, C. *Bisphosphonates in Medical Practice*, 1st ed.; Springer: Berlin/Heidelberg, Germany, 2007; pp. 23–68.
5. Watts, N.B.; Diab, D.L. Long-Term Use of Bisphosphonates in Osteoporosis. *J. Clin. Endocrinol. Metab.* **2021**, *95*, 1555–1565. [[CrossRef](#)]
6. Sandomierski, M.; Zielińska, M.; Voelkel, A. A long-term controlled release of the drug for osteoporosis from the surface of titanium implants coated with calcium zeolite. *Mater. Chem. Front.* **2021**, *5*, 5718–5725. [[CrossRef](#)]
7. Park, K.W.; Yun, Y.P.; Kim, S.E.; Song, H.R. The Effect of Alendronate Loaded Biphasic Calcium Phosphate Scaffolds on Bone Regeneration in a Rat Tibial Defect Model. *Int. J. Mol. Sci.* **2015**, *16*, 26738–26753. [[CrossRef](#)]
8. Spinthaki, A.; Matheis, J.; Hater, W.; Demadis, K.D. Antiscalant-driven inhibition and stabilization of “magnesium silicate” under geothermal stresses: The role of magnesium-phosphonate coordination chemistry. *Energy Fuels* **2018**, *32*, 11749–11760. [[CrossRef](#)]
9. Mozafari, M. *Metal-Organic Frameworks for Biomedical Applications*; Elsevier: Amsterdam, The Netherlands, 2020.
10. Barbosa, J.S.; Pinto, M.; Barreiro, S.; Fernandes, C.; Mendes, R.F.; Lavrador, P.; Gaspar, V.M.; Mano, J.F.; Borges, F.; Remião, F.; et al. Coordination Compounds As Multi-Delivery Systems for Osteoporosis. *ACS Appl. Mater. Interfaces* **2021**, *13*, 35469–35483. [[CrossRef](#)]
11. Vassaki, M.; Papathanasiou, K.E.; Hadjicharalambous, C.; Chandrinou, D.; Turhanen, P.; Choquesillo-Lazarte, D.; Demadis, K.D. Self-Sacrificial MOFs for Ultra-Long Controlled Release of Bisphosphonate Anti-Osteoporotic Drugs. *Chem. Commun.* **2020**, *56*, 5166–5169. [[CrossRef](#)]
12. Nancollas, G.H.; Tang, R.; Phipps, R.J.; Henneman, Z.; Gulde, S.; Wu, W.; Mangood, A.; Russell, R.G.G.; Ebetino, F.H. Novel insights into actions of bisphosphonates on bone: Differences in interactions with hydroxyapatite. *Bone* **2006**, *38*, 617–627. [[CrossRef](#)]
13. Bruker APEX3. *APEX3 V2019.1*; Bruker-AXS: Madison, WI, USA, 2019.
14. Sheldrick, G.M. SHELXT—Integrated Space-Group and Crystal-Structure Determination. *Acta Crystallogr. Sect. A Found. Crystallogr.* **2015**, *71*, 3–8. [[CrossRef](#)]
15. Sheldrick, G.M. Crystal Structure Refinement with SHELXL. *Acta Crystallogr. Sect. C Struct. Chem.* **2015**, *71*, 3–8. [[CrossRef](#)]
16. Dolomanov, O.V.; Bourhis, L.J.; Gildea, R.J.; Howard, J.A.K.; Puschmann, H. OLEX2: A Complete Structure Solution, Refinement and Analysis Program. *J. Appl. Crystallogr.* **2009**, *42*, 339–341. [[CrossRef](#)]
17. Macrae, C.F.; Bruno, I.J.; Chisholm, J.A.; Edgington, P.R.; McCabe, P.; Pidcock, E.; Rodriguez-Monge, L.; Taylor, R.; van de Streek, J.; Wood, P.A. Mercury CSD 2.0—New Features for the Visualization and Investigation of Crystal Structures. *J. Appl. Crystallogr.* **2008**, *41*, 466–470. [[CrossRef](#)]
18. Kieczkowski, G.R.; Jobson, R.B.; Melillo, D.G.; Reinhold, D.F.; Grenda, V.J.; Shinkai, I. Preparation of (4-Amino-1-Hydroxybutylidene) bisphosphonic Acid Sodium Salt, MK-217 (Alendronate Sodium). An Improved Procedure for the Preparation of 1-Hydroxy-1,1-bisphosphonic Acids. *J. Org. Chem.* **1995**, *60*, 8310–8312. [[CrossRef](#)]
19. Gossman, W.L.; Wilson, S.R.; Oldfield, E. Three hydrates of the bisphosphonate risedronate, consisting of one molecular and two ionic structures. *Acta Cryst.* **2003**, *C59*, m33–m36. [[CrossRef](#)] [[PubMed](#)]
20. Neofotistou, E.; Demadis, K.D. Silica Scale Growth Inhibition by Polyaminoamide STARBURST® Dendrimers. *Coll. Surf. A Physicochem. Eng. Asp.* **2004**, *242*, 213–216. [[CrossRef](#)]
21. Demadis, K.D. A Structure/Function Study of Polyaminoamide (PAMAM) Dendrimers as Silica Scale Growth Inhibitors. *J. Chem. Technol. Biotechnol.* **2005**, *80*, 630–640. [[CrossRef](#)]
22. Demadis, K.D.; Neofotistou, E. Synergistic Effects of Combinations of Cationic Polyaminoamide Dendrimers/Anionic Polyelectrolytes on Amorphous Silica Formation: A Bioinspired Approach. *Chem. Mater.* **2007**, *19*, 581–587. [[CrossRef](#)]
23. Demadis, K.D.; Neofotistou, E. Inhibition and Growth Control of Colloidal Silica: Designed Chemical Approaches. *Mater. Perform.* **2004**, *43*, 38–42.
24. Neofotistou, E.; Demadis, K.D. Cationic Polymeric Chemical Inhibitors and Multifunctional Blends for the Control of Silica Scale in Process Waters. *Int. J. Corros. Scale Inhib.* **2014**, *3*, 28–34. [[CrossRef](#)]
25. Neofotistou, E.M.A.S.E.; Demadis, K.D. Environmentally benign chemical additives in the treatment and chemical cleaning of process water systems: Implications for green chemical technology. *Desalination* **2007**, *210*, 257–265.

26. Barbey, C.; Lecouvey, M. Crystal structure of (1-hydroxy-1-phosphono-2-pyridin-3-yl-ethyl)-phosphonic acid (risedronate), C₇H₁₁NO₇P₂·H₂O, an antiresorptive bones drug. *Z. Kristallogr.* **2002**, *217*, 137–138.
27. Stahl, K.; Oddershede, J.; Preikschat, H.; Fischer, E.; Bennekou, J.S. Ammonium 1-hydroxy-2-(2-pyridinio)ethane-1,1-diyl-diphosphonate dihydrate and potassium 1-hydroxy-2-(2-pyridinio)ethane-1,1-diyl-diphosphonate dihydrate. *Acta Cryst.* **2006**, *C62*, m112–m115.
28. Ma, K.-R.; Zhang, Y.; Kan, Y.-H.; Yang, X.-J.; Cong, M.-H. Three M(II)-diphosphonate coordination polymers with N-heterocyclic group (M = Ni, Fe, Mg): Synthesis, characterization and magnetic properties. *Synth. Met.* **2013**, *182*, 40–48. [[CrossRef](#)]
29. Demoro, B.; Caruso, F.; Rossi, M.; Benítez, D.; Gonzalez, M.; Cerecetto, H.; Parajón-Costa, B.; Castiglioni, J.; Galizzi, M.; Docampo, R.; et al. Risedronate metal complexes potentially active against Chagas disease. *J. Inorg. Biochem.* **2010**, *104*, 1252–1258. [[CrossRef](#)]
30. Ma, K.-R.; Cao, L.; Cong, M.-H.; Kan, Y.-H.; Li, R.-Q. Three pyridyl modified Cu(II)/Cd(II)-diphosphonates: Syntheses, crystal structures and properties. *J. Mol. Struct.* **2017**, *1139*, 67–77. [[CrossRef](#)]
31. Papathanasiou, K.E.; Vassaki, M.; Spinthaki, A.; Alatzoglou, F.-E.G.; Tripodianos, E.; Turhanen, P.; Demadis, K.D. Phosphorus chemistry: From small molecules to polymers to pharmaceutical and industrial applications. *Pure Appl. Chem.* **2019**, *91*, 421–441. [[CrossRef](#)]
32. Papathanasiou, K.E.; Turhanen, P.; Brückner, S.I.; Brunner, E.; Demadis, K.D. Smart, programmable and responsive injectable hydrogels for controlled release of cargo osteoporosis drugs. *Sci. Rep.* **2017**, *7*, 4743. [[CrossRef](#)]